Journal of Alloys and Compounds 480 (2009) 315–320

Contents lists available at ScienceDirect

Journal of Alloys and Compounds

journal homepage: www.elsevier.com/locate/jallcom

Combustion synthesis of Ti(C, N)–TiB_2 from a Ti–C–BN system

Lei Zhan, Ping Shen, Shenbao Jin, Qichuan Jiang*

Key Laboratory of Automobile Materials, Department of Materials Science and Engineering, Jilin University, No. 5988 Renmin Street, Changchun, 130025, PR China

ARTICLE INFO

Article history:
Received 8 December 2008
Received in revised form 15 January 2009
Accepted 25 January 2009
Available online 6 February 2009

Keywords:
Titanium carbonitrides
SHS
Ceramics

ABSTRACT

In this paper, a simple way of fabricating TiC_xN_y–TiB_2 ceramics through the combustion reaction of Ti, C and BN powder mixtures in an argon atmosphere is reported with an emphasis on the effects of the C/(C + N) ratio on the SHS reaction behaviors and mechanism. With the increase in the C/(C + N) ratio, the combustion temperature shows a zigzag variation behavior; the combustion wave velocity displays a similar variation tendency as did in the combustion temperature while the ignition delay time increases progressively. XRD results confirmed that TiC_xN_y–TiB_2 could form in all the samples. Microstructural observations revealed that both TiC_xN_y and TiB_2 grains had fine sizes of less than 1 μm in the products when the C/(C + N) ratio was lower than 0.5. Based on the characterization of quenched samples, the formation mechanism of the titanium carbonitride is proposed. Namely, the formations of $TiN_{0.3}$ and TiN are followed by the incorporation of C in TiN_x to form the titanium carbonitride solid solution.

1. Introduction

Titanium carbonitride, Ti(C, N) (the stoichiometric phase can be expressed as TiC_xN_y with $x + y = 1$), was developed from TiC matrix cermets by addition of TiN in the 1970s [1]. Because of its outstanding physical properties, such as high hardness, high corrosion resistance and high thermodynamic stability, Ti(C, N) has been successfully used in cutting tools and wear-resistance materials when combined with metal binders, such as Ni, Co and Mo [2–5]. Furthermore, the addition of different ceramic phases (e.g., WC, Mo_2C, TiN and TiC) into Ti(C, N) matrix could effectively improve the physical and mechanical properties of cermets to meet the requirement of the cutting task [3,6–8].

Usually, Ti(C, N) powders were produced by the carbothermal reduction of titania (TiO_2) in nitrogen [9,10]. However, the appearance of TiO_2, Ti_xO_y, C, etc. in the final product lowers the purity of the Ti(C, N) powders produced from the reduction reaction. In addition, chemical vapor deposition (CVD) was also applied to synthesize the Ti(C, N) coatings, even though it is costly [11]. In recent years, self-propagating high-temperature synthesis (SHS) or combustion synthesis (CS) with the advantages of time- and energy-saving has been a promising route to produce advanced materials, including carbides, nitrides, and carbonitrides [12–14]. Carole et al. [12] and Yeh and Chen [13], respectively, synthesized Ti(C, N) from a Ti–C system by SHS in gaseous nitrogen. Eslamloo-Grami and Munir [15], on the other hand, investigated the mechanism of synthesis of Ti(C, N) by titanium, carbon and nitrogen gas. However, the reported combustion synthesis processes are generally carried out at high nitrogen pressure, which is not desirable from a safety point of view. On the other hand, the gas pressure has a great effect on the degree of nitrogen conversion of the Ti–C mixtures and the heterogeneous products from surface to center of the sample are unavoidable [3].

More recently, the use of solid source of nitrogen, such as BN and Si_3N_4, as a reactant has been demonstrated to be effective in combustion synthesis of nitrides [16–18]. Accordingly, we proposed the following reaction for the synthesis of the Ti(C, N) ceramic:

$$\frac{2+y}{2}\mathrm{Ti} + x\mathrm{C} + y\mathrm{BN} \rightarrow \mathrm{TiC}_x\mathrm{N}_y + \frac{y}{2}\mathrm{TiB}_2 \quad (1)$$

It is expected that a desirable product of Ti(C, N) could be readily obtained by using the SHS process. Using BN as a reactant in the above reaction not only provides a solid source of nitrogen to solve the problem of permeation-limited reactions with gaseous nitrogen, but also leads to the formation of TiB_2, which is also a refractory material with many attractive properties, such as high melting point, high hardness, good electrical conductivity and excellent wear and corrosion resistance [19]. In this work, we report the synthesis of Ti(C, N)–TiB_2 ceramics by combustion reaction in the Ti–C–BN system with an emphasis on the effects of the C/(C + N) ratio in the reactants on the SHS reaction behaviors and mechanism in the Ti–C–BN system. It is expected that the understanding of the reaction behaviors and products would not only permit a better control of the reaction process through the regulation of processing parameters, but also provide a guide for producing the Ti(C, N)–TiB_2 composites with tailored microstructures and properties.

* Corresponding author. Tel.: +86 431 85094699; fax: +86 431 85094699.
E-mail address: jqc@jlu.edu.cn (Q.C. Jiang).

0925-8388/$ – see front matter © 2009 Elsevier B.V. All rights reserved.
doi:10.1016/j.jallcom.2009.01.087

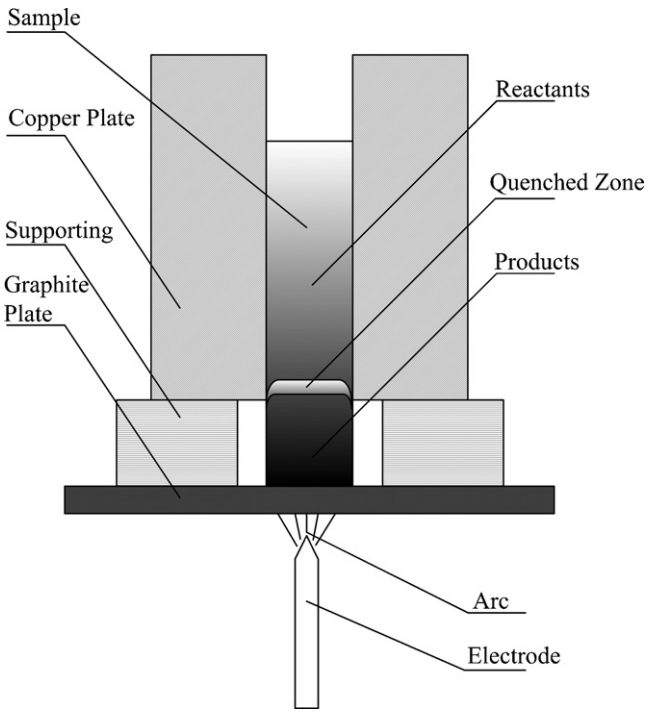

Fig. 1. Schematic representation of the quench sample.

2. Experimental procedure

Commercial powders of Ti, BN and C were used as starting materials. Details about the characteristics of the starting powders with their sources are presented in Table 1. Based on reaction (1), the powder blends with five different molar ratios of C/(C + N) (i.e., 0.1, 0.3, 0.5, 0.7 and 0.9, respectively) were prepared for the synthesis of the Ti(C, N)–TiB_2 ceramics. The powders were dry-mixed for 8 h and then hand-blended for 30 min to ensure homogeneity. After mixing, the powders with suitable weights were uniaxially pressed into cylindrical specimens (22 mm in diameter and 12 mm in height) with relative densities of 70 ± 5%, as determined from weight and geometric measurements.

The SHS experiments were conducted in a combustion chamber under a protective atmosphere of industrial argon (99.9%). The green specimen was placed on a graphite plate with a thickness 4 mm and ignited from the bottom by arc heating using a current of 75 A. The combustion temperatures were measured by W–5%Re/W–26%Re thermocouples embedded into the sample with about 5 mm in depth and the signals were recorded and processed by a data acquisition system using an acquisition speed of 50 ms/point. The combustion process was recorded by a CCD video camera at a scanning speed of 72 frames/s to evaluate the combustion wave velocity. The phase compositions of the reacted samples were analyzed by X-ray diffraction (XRD, Rigaku-D/Max 2500PC, Japan) using Cu Kα radiation. In order to eliminate residual stress in the synthesized products, which could have an effect on the lattice parameter calculation for the synthesized TiC_xN_y, the samples were crushed into powders for the XRD analysis. Microstructures at the fracture surface of the reaction products were observed by field emission scanning electron microscopy (FESEM, JSM 6700F, Japan).

To investigate the mechanism of phase formation during synthesis, an quenching of the combustion wave during its passage through the compacts was carried out for the samples with C/(C + N) = 0.1, 0.5 and 0.9, respectively. The mixed powders were compacted into rectangular bars in dimensions of 65 mm × 10 mm × 6 mm with a relative green density of ~75% and then placed on a graphite plate with two copper plates on its sides as shown in Fig. 1. The resulting planar wave propagated for several seconds, but became extinguished at the sample–copper plate interface. The unreacted part, the quenched zone and the combustion synthesized products in the quenched samples were carefully examined by X-ray micro-diffraction (D8 Discover with GADDS, Bruker AXS, Karlsruhe, Germany) using an 800 μm beam diameter.

3. Results and discussion

3.1. Reaction behaviors and products

Fig. 2(a) shows the dependence of the maximum combustion temperatures, T_c, on the molar ratio of C/(C + N) in the reactants. As indicated, the measured combustion temperature increases as the C/(C + N) ratio increases from 0.1 to 0.5 in the reactants. As the C/(C + N) ratio further increases from 0.5 to 0.9, the combustion temperature shows a first decrease and then increase. It should be mentioned that the measured combustion temperatures are usually beyond 2300 °C and are determined by extrapolation from the available temperature–electromotive force function, which might have a relatively large error. In a strict sense, the values indicated in Fig. 2(a) show only the variation tendency with the increase in the reactant C/(C + N) ratio.

Since we could not find available thermodynamic data such as the heat capacities and the enthalpies of formation and fusion for TiC_xN_y, here the analysis is based on the combination of TiC and TiN. The reactions between the reactants in the Ti–C–BN system are as follows:

$$3Ti + 2BN \rightarrow TiB_2 + 2TiN \quad (2)$$

$$Ti + C \rightarrow TiC \quad (3)$$

The adiabatic combustion temperatures (T_{ad}) of reactions (2) and (3) were calculated using the thermodynamic data from Ref. [20]. The calculated results indicated that the values of T_{ad} are 2997 and 3017 °C, respectively, suggesting that the maximum combustion temperature would increase with the increasing C/(C + N) ratio due to the increase in the amount of TiC in the products. However, this was not the case in the current study. Such a behavior may be the result of the change in the reaction mode. That is, reaction (2) might be dominant at low C/(C + N) ratios, while reaction (3) is dominant at high C/(C + N) ratios.

In order to validate the above speculation, the system of Ti–BN associating with the following reaction:

$$(3+x)Ti + 2BN \rightarrow TiB_2 + 2TiN + xTi \quad (4)$$

was investigated. The dependence of the adiabatic temperature of reaction (4) on the BN/Ti ratio [i.e., $2/(3+x)$ $(x \geq 0)$] was calculated and the results are shown in Fig. 2(b). As can be seen, a remarkable increase in temperature appears with an increase in the BN/Ti ratio. According to Merzhanov's empirical criterion, i.e., T_{ad} should not be lower than 1800 K (1527 °C) [21] for a reaction to be self-sustaining without preheat, the molar ratio of BN/Ti should be higher than 0.2657. In addition, Eslamloo-Grami and Munir [15] indicated no self-sustaining reaction in the Ti–C system unless C/Ti = 0.3 or higher. Following these hints, variations in the molar ratios of BN/Ti and C/Ti with the C/(C + N) ratio in the reactants were calculated and the results are shown in Fig. 2(c). As indicated, three regions could be distinguished in Fig. 2(c). In region I [i.e., C/(C + N) ≤ 0.39], the C/Ti ratio varies between 0 and 0.3, implying that the combustion temperature depends greatly on the reaction between Ti and BN. In region II [i.e., 0.39 < C/(C + N) < 0.694], the self-sustaining reaction could occur in both Ti–C and Ti–BN systems, and in region III [i.e., C/(C + N) ≥ 0.694], the BN/Ti ratio is in the range of 0–0.2657, while the C/Ti ratio changes from 0.59 to 1.0, implying that the SHS process is mainly controlled by the reaction between

Table 1
The characteristics of the reactant powders used in this study.

Reactant	Purity (wt.%)	Particle size (μm)	Source
Ti	>99.5	~38	Institute of Nonferrous Metals, Pekin, China
C	>99.0	~48	Sinosteel Jilin Carbon Co., Ltd., Jilin, China
BN	>99.0	~3.0	Ying Kou Liaobin Fine Chemicals Co., Ltd., Yingkou, China

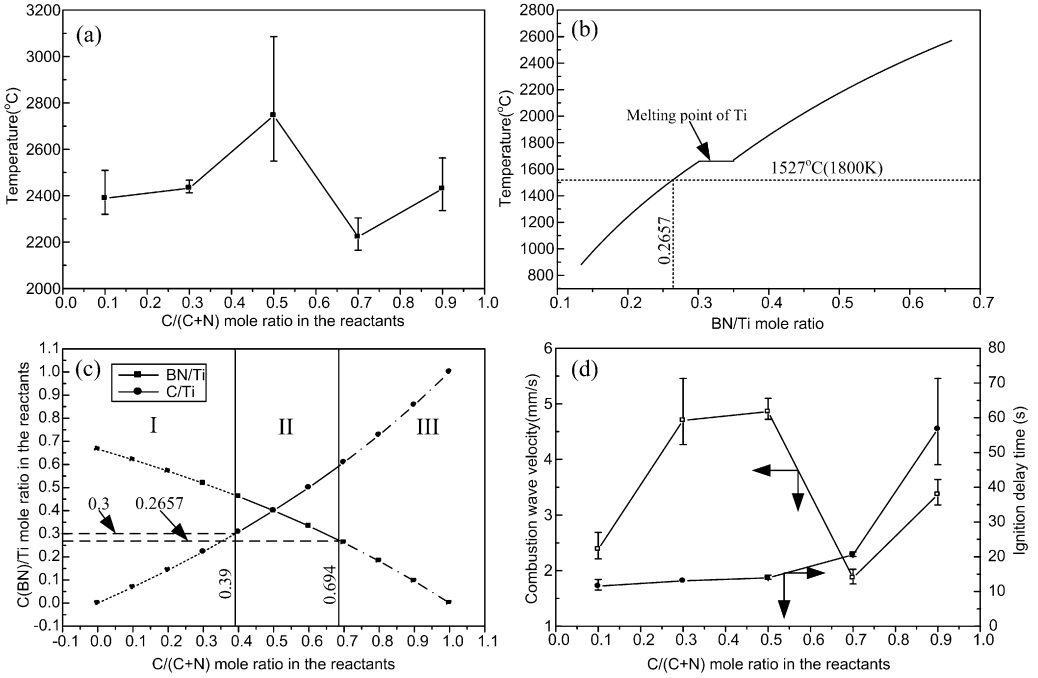

Fig. 2. (a) Variations in the maximum combustion temperature with the C/(C + N) ratio in the reactants, (b) variations in the calculated adiabatic combustion temperature of Ti–BN system with molar ratio of BN/Ti, (c) variations in the molar ratios of BN/Ti and C/Ti in the green specimens with the C/(C + N) ratio in the reactants and (d) variations in the ignition delay time and the combustion wave velocity with the C/(C + N) ratio in the reactants.

Ti and C. Clearly, for C/(C + N) < 0.5, the heat produced by the reaction between Ti and BN is sufficient for the self-sustaining of the reaction in the Ti–C–BN system. After occurrence of the reaction between Ti and BN, the heat produced from the reaction promotes the reaction between Ti and C, which is more exothermic. As a result, the combustion temperature shows an increase with the increase in the C/(C + N) ratio. For C/(C + N) > 0.5, the SHS process was gradually controlled by the reaction between Ti and C. Due to the coarse C particles were used in this work, the reaction between Ti and BN occurred prior to Ti and C, yielding prior formation of TiN_x, as will be discussed in Section 3.2. With the increase of the C/(C + N) ratio, the decrease in the BN content greatly decreased the heat released from the reaction between Ti and BN. When the C/(C + N) ratio increased to 0.7, the heat released from the reaction between Ti and BN could not ignite the self-sustaining reaction in the Ti–C–BN system, while a long time heating was needed [see Fig. 2(d)]. Consequently, before the formation of the titanium carbonitride solid solution, the TiN_x phase preferentially formed during the reaction might act as reaction diluents, leading to the decrease in the combustion temperature. With the further increasing C/(C + N) ratio, the decrease in the amount of TiN_x weakened the dilution effect. Therefore, the combustion temperature increased again. On the other hand, as the C/(C + N) increased from 0.7 to 0.9, the C/Ti ratio in the reactants ranged from 0.6 to 0.857. According to Holt and Munir [21] and Yang et al. [22], the combustion temperature of the Ti–C system increased as the C/Ti ratio increased from 0.6 to 1.0. Consequently, the combustion temperature increased again.

Fig. 2(d) shows the variations in combustion wave velocity (V_{wave}) and ignition delay time (t_{ig}) with the C/(C + N) ratio. As shown, with the increase in the C/(C + N) ratio, V_{wave} exhibits a similar variation tendency as did in the combustion temperature, while the ignition delay time increases progressively. It is known that the wave velocity depends largely on the combustion temperature and the thermal conductivity of the compact. It is believed that the thermal conductivity of solid C at room temperature is the highest among the three constituents Ti, C and BN. With the increase in the C/(C + N) ratio, the thermal conductivity of the compact increases due to the high thermal conductivity of C. If without consideration of the combustion temperature, the wave velocity should increase. Therefore, the present experimental results demonstrate that the combustion temperature plays a more important role in the propagation velocity of the combustion wave than the thermal conductivity of the compact.

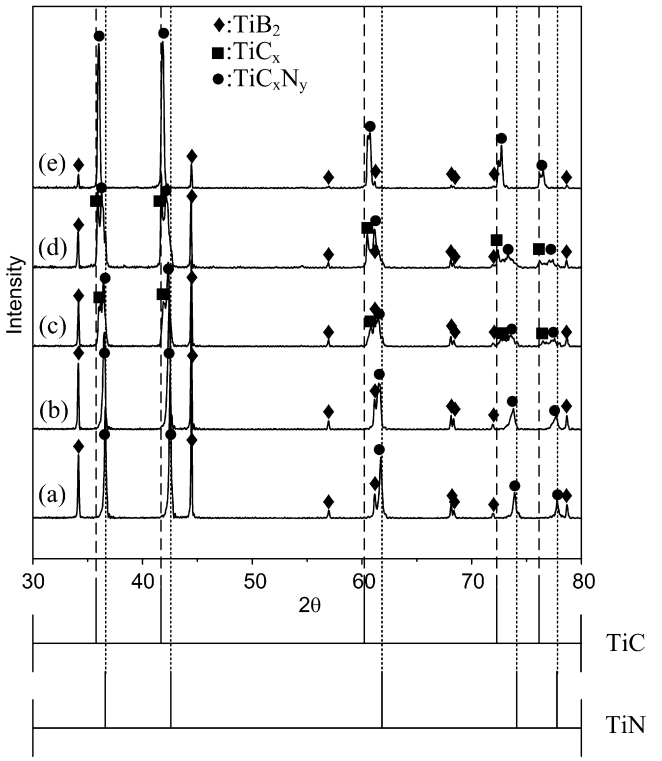

Fig. 3. XRD patterns of the synthesized products with various C/(C + N) ratios in the reactants: (a) 0.1, (b) 0.3, (c) 0.5, (d) 0.7 and (e) 0.9.

The time from the start of heating to the occurrence of SHS reaction is called ignition time. It is interesting to note that the ignition time shows a considerable increase with the increase in the C/(C + N). The reaction mechanism, as will be discussed in Section 3.2, informed us that the reaction between Ti and BN occurs prior to Ti and C due to the use of the coarse C particles in the reactants. With the increase in the C/(C + N) ratio, the decrease in the BN content in the reactants led to a decrease in the heat released from the reaction between Ti and BN. As a result, the self-sustaining reaction in the Ti–C–BN system could not occur until the occurrence of the reaction between Ti and C. Therefore, it is not difficult to understand that the sample with high C/(C + N) ratio was difficult to ignite, resulting in an increase in the ignition delay time.

Fig. 3 shows the XRD patterns of the SHS reaction products synthesized by green compacts with the molar ratios of C/(C + N) = 0.1, 0.3, 0.5, 0.7 and 0.9, respectively, compared with the standard patterns for TiN and TiC [23,24]. As indicated, the phase compositions of the final products in the five samples are nearly the same, consisting mainly of TiB_2 and TiC_xN_y as designed together with some TiC_x. The presence of the TiC_x phase in the products is noticeable for the samples with C/(C + N) = 0.5 and 0.7. In this work, the carbonitride solid solution could form through two ways: (a) the C atoms diffused directly into the titanium nitride cell and (b) elemental C reacted with Ti to form the titanium carbide product, which in turn reacted with TiN_x to form the titanium carbonitride solid solution. As the SHS reaction finished in a short time, a small quantity of TiC_x could not combine with TiN_x to form the titanium carbonitride solid solution and was retained in the final products.

Fig. 4 shows the representative FESEM images of the microstructures at the fracture surfaces of the reacted samples with different C/(C + N) ratios. In the samples synthesized from the Ti–C–BN system, it is somewhat difficult to distinguish TiC_xN_y and TiB_2 from their morphologies. Generally, TiB_2 exhibited an abnormal grain growth with typical hexagonal prism shapes [25–27], but this was not the case in the current study. As indicated in Fig. 4, some particles with fine platelet shapes seem to intermix with many equiaxed ceramic particles. The characteristic grain sizes of these ceramic phases are about 1 μm when the C/(C + N) ratio is no more than 0.5. Such fine microstructures could be attributed to the low amount of liquid during the SHS reaction, which provided limited space for the grain growth. In addition, the sizes of these ceramic particles, especially for those with platelet shapes, increase considerably as the C/(C + N) ratio increases up to 0.5. This can be explained by the fact that the crystal growth depends primarily on the combustion temperature. In the case of the sample with C/(C + N) = 0.9, however, the ceramic particulates exhibit larger grain sizes than those in the samples with low C/(C + N) ratios [Fig. 4(d)] and some growth steps on the ceramic particulates can be clearly observed [see the insert in Fig. 4(d)]. A similar morphology of the growth steps was also

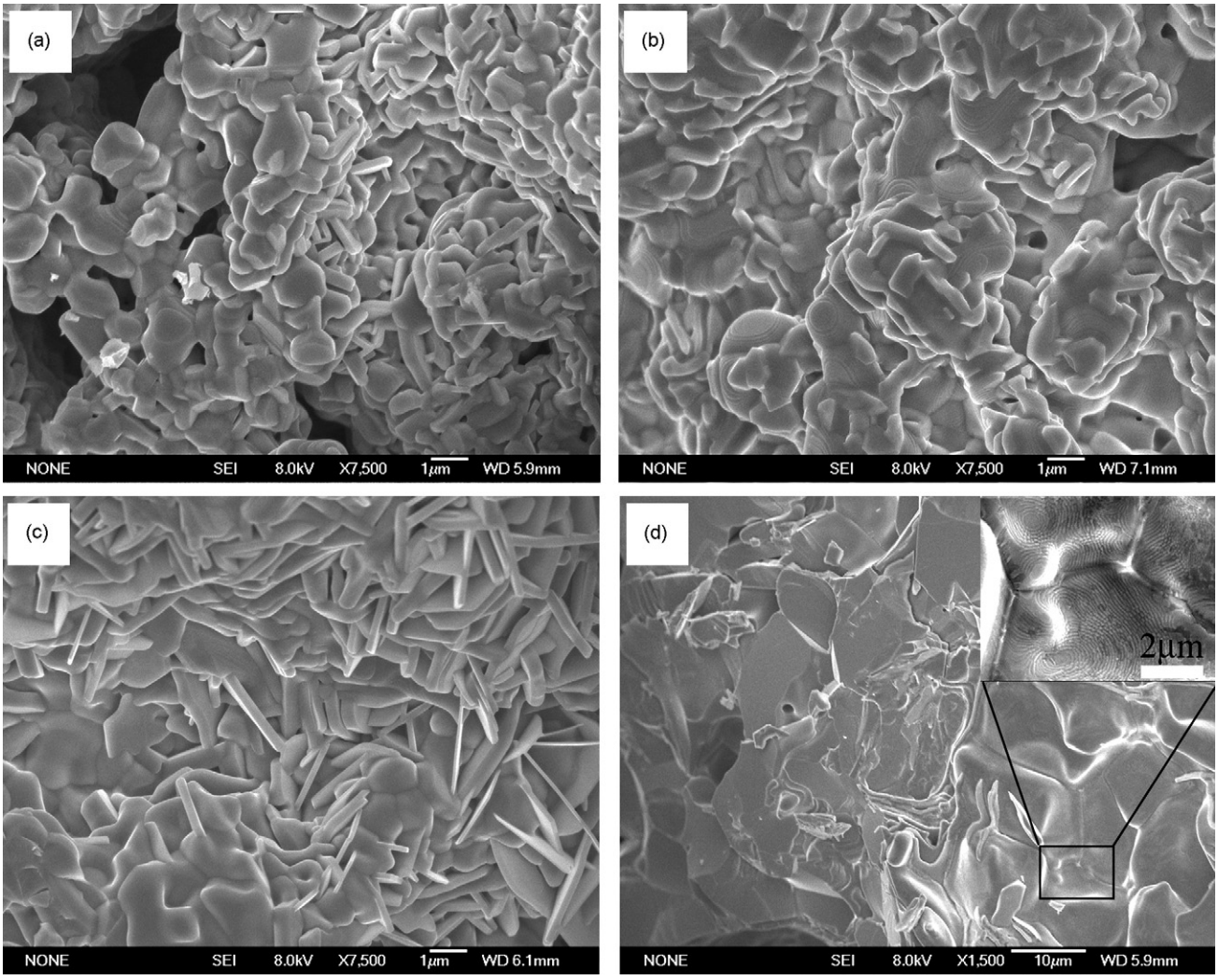

Fig. 4. Representative microstructures at the fracture surfaces of the SHS samples with different C/(C + N) ratios in the reactants: (a) 0.1, (b) 0.3, (c) 0.5 and (d) 0.9.

observed in the combustion-synthesized TiC particulates using the Al–Ti–C system [28].

3.2. Reaction mechanisms

The preceding results indicate that the reaction behaviors and the final products of the Ti–C–BN system are greatly dependent on the C/(C + N) ratio in the reactants. In order to clarify the reaction mechanism in the samples, the combustion front quenching was performed in the samples with C/(C + N) = 0.1, 0.5 and 0.9, respectively. Figs. 5 and 6 show the X-ray micro-diffraction patterns of the phases in the different regions of the samples with C/(C + N) = 0.5 and 0.9, respectively. It is worth mentioning that the phase evolution history in the sample with C/(C + N) = 0.1 was similar to that in the sample with C/(C + N) = 0.5, and thus it was not presented here.

According to Fig. 5, the phase evolution history in the samples with C/(C + N) = 0.9 could be described as

$$(1)\mathrm{Ti} + \mathrm{C} + \mathrm{BN} \rightarrow (2)\mathrm{Ti} + \mathrm{C} + \mathrm{BN} + \mathrm{TiN}_{0.3} + \mathrm{TiN} \rightarrow (3)\mathrm{Ti} + \mathrm{C} + \mathrm{BN} + \mathrm{TiN}_{0.3} + \mathrm{TiN} + \mathrm{TiC}_{0.3}\mathrm{N}_{0.7} \rightarrow (4)\mathrm{Ti} + \mathrm{C} + \mathrm{BN} + \mathrm{TiN} + \mathrm{TiC}_{0.3}\mathrm{N}_{0.7} \rightarrow (5)\mathrm{Ti} + \mathrm{C} + \mathrm{BN} + \mathrm{TiC}_{0.3}\mathrm{N}_{0.7} + \mathrm{TiB} \rightarrow (6)\mathrm{Ti} + \mathrm{C} + \mathrm{TiB} + \mathrm{TiB}_{2+TiC_xN_y} \rightarrow (7)\mathrm{TiC}_x\mathrm{N}_y + \mathrm{TiB}_2$$

We can see that (i) the $TiN_{0.3}$ and TiN phases form prior to any other new phases in the current study, and then they transform to

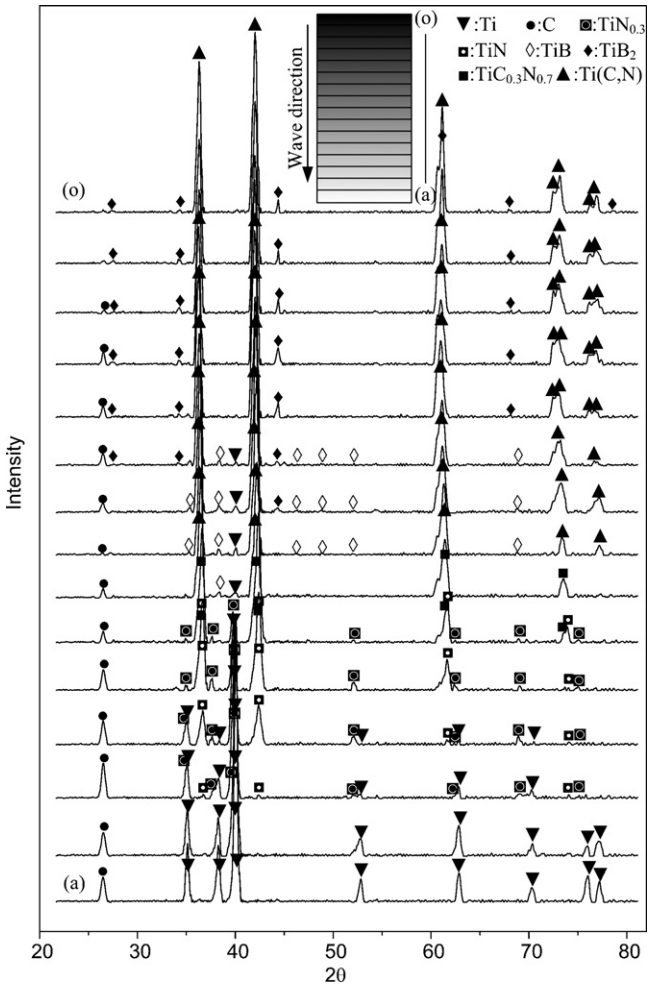

Fig. 5. X-ray micro-diffraction patterns for the quenched sample with C/(C + N) = 0.9 in the differently reacted regions: (a → b) reactant region, (c → f) preheated region, (g → m) combustion region, and (n → o) reacted region.

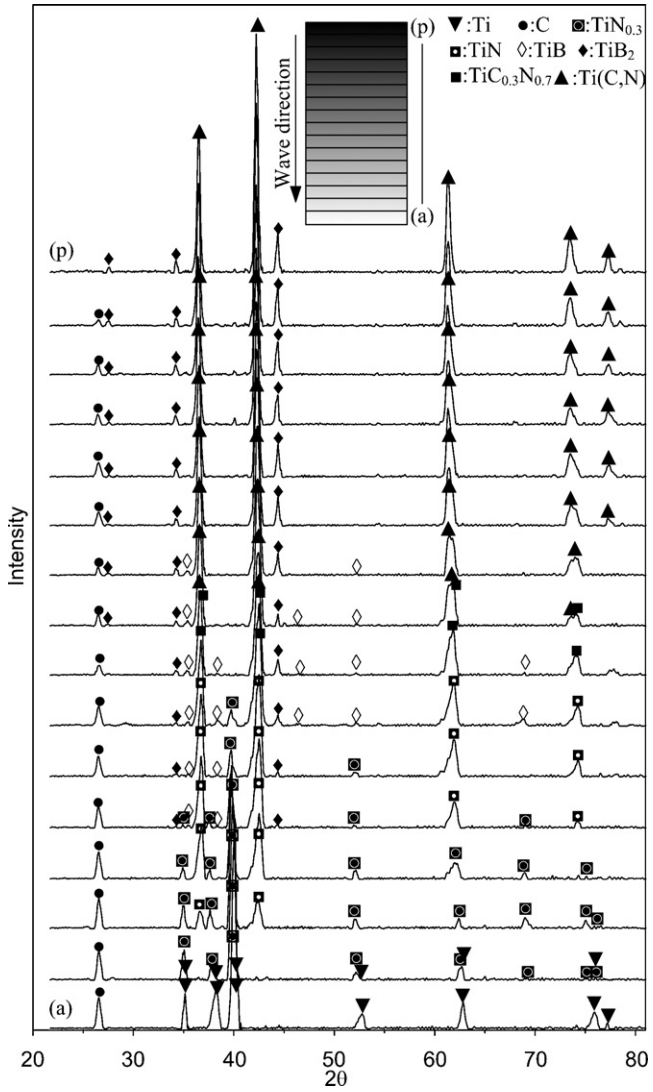

Fig. 6. X-ray micro-diffraction patterns for the quenched sample with C/(C + N) = 0.5 in the differently reacted regions: (a) reactant region, (b → e) preheated region, (f–n) combustion region, and (o–p) reacted region.

TiC_xN_y through the incorporation of the C atoms in TiN_x. On the other hand, as the reaction advanced, BN was greatly consumed by the formation of TiN_x, while a larger amount of Ti and C was retained, yielding the TiC_x phase at high temperatures and then TiC_x combined with TiN_x to form the titanium carbonitride solid solution; (ii) as the reaction proceed, the boron (B) atoms were remained due to the escape of the nitrogen (N) atoms from bulk BN and then bonded with Ti to form TiB. Actually, the TiB phase in the reaction zone could be melted as the combustion wave arrived (According to the phase diagram of Ti–B [29], a eutectic reaction between TiB and Ti occurs at 1540 °C. The heat released from the reactions during the SHS process can lead to the formation of Ti–B eutectic liquid). Therefore, once the concentration of B in the Ti–B melt became saturate, the TiB_2 particulates would precipitate; (iii) the diffraction peaks of TiC_xN_y substantially shifted to a lower angle. This can be explained by the atomic radii of elements: carbon radius is 0.91 Å and nitrogen radius is 0.75 Å. A substitution of nitrogen by carbon would result in an increase in the cell size and thus a shift of the peaks to lower angles in the diffraction pattern; (iv) finally, in the reacted region, the product consisted of TiB_2 and TiC_xN_y, indicating a fairly complete reaction.

Similarly, the reaction sequence in the sample with C/(C + N) = 0.5 [see Fig. 6] could be written as

$$(1)\mathrm{Ti} + \mathrm{C} + \mathrm{BN} \rightarrow (2)\mathrm{Ti} + \mathrm{C} + \mathrm{BN} + \mathrm{TiN}_{0.3} \rightarrow (3)\mathrm{C} + \mathrm{BN} + \mathrm{TiN}_{0.3} + \mathrm{TiN} \rightarrow (4)\mathrm{C} + \mathrm{BN} + \mathrm{TiN} + \mathrm{TiN}_{0.3} + \mathrm{TiB} + \mathrm{TiB}_2 \rightarrow (5)\mathrm{C} + \mathrm{TiN} + \mathrm{TiB} + \mathrm{TiB}_2 \rightarrow (6)\mathrm{C} + \mathrm{TiB} + \mathrm{TiB}_2 + \mathrm{TiC}_{0.3}\mathrm{N}_{0.7} \rightarrow (7)\mathrm{C} + \mathrm{TiB} + \mathrm{TiB}_2 + \mathrm{TiC}_{0.3}\mathrm{N}_{0.7} + \mathrm{TiC}_x\mathrm{N}_y \rightarrow (8)\mathrm{C} + \mathrm{TiC}_x\mathrm{N}_y + \mathrm{TiB} + \mathrm{TiB}_2 \rightarrow (9)\mathrm{C} + \mathrm{TiB}_2 + \mathrm{TiC}_x\mathrm{N}_y \rightarrow (10)\mathrm{TiB}_2 + \mathrm{TiC}_x\mathrm{N}_y$$

Compared with that in the sample with C/(C + N) = 0.9, the reactions were similar in the initial stages, i.e., the prior formation of $TiN_{0.3}$ and TiN and then appearance of the TiB, TiB_2 and $TiC_{0.3}N_{0.7}$ phases. However, the formation sequence of the titanium borides (i.e., TiB, TiB_2) and $TiC_{0.3}N_{0.7}$ phases in the sample with C/(C + N) = 0.9 is somewhat different from that in the sample with C/(C + N) = 0.5. For C/(C + N) = 0.9, the high concentration of C in the reactants greatly enlarged the contact opportunity and area between C and Ti. As a result, the diffusion of the C atoms into the titanium nitride cell became easy while the formation of the Ti–B compounds turned difficult due to the lower concentration of B, which diffused away from the BN crystal. For C/(C + N) = 0.5, however, the quantity of C substantially decreased while that of BN increased. After the formation of TiN_x, a larger amount of B atoms were retained and rapidly bonded with Ti to form the Ti–B compounds. Therefore, the TiB and TiB_2 phases formed prior to $TiC_{0.3}N_{0.7}$.

Accordingly, we deem that the reaction mechanisms, in a general sense, do not differ significantly in the Ti–C–BN systems with the low and high C/(C + N) ratios. The reactions in both cases commenced with the prior formation of $TiN_{0.3}$ and TiN and then proceeded with the incorporation of the C atoms in the titanium nitride cell to form the titanium carbonitride solid solution. The difference in the high and low C/(C + N) ratio samples is in the formation sequence of the $TiC_{0.3}N_{0.7}$ and TiB phases. In the samples with the high C/(C + N) ratios, $TiC_{0.3}N_{0.7}$ forms prior to TiB due to the high concentration of C while it turns over in the samples with the low C/(C + N) ratios. On the other hand, this reaction mechanism is apparently different from that in the Ti–C–N_2 system [15]. Eslamloo-Grami and Munir [15], who produced titanium carbonitride by combustion reaction between titanium and carbon in a nitrogen atmosphere, indicated the following reaction steps:

$$\mathrm{Ti} + 0.5\mathrm{C} \rightarrow \mathrm{TiC}_{0.5} \quad (4)$$

$$\mathrm{TiC}_{0.5} + 0.25\mathrm{N}_2 \rightarrow \mathrm{TiC}_{0.5}\mathrm{N}_{0.5} \quad (5)$$

The discrepancy in the reaction mechanism could be due to the difference in the nitrogen source as well as the coarse C particles used in the experiments. With regard to the influence of the particle sizes of C and BN, it should be mentioned here that the reaction mechanism deduced in this work only applied to the Ti–C–BN system, with the coarse C and fine BN particles in the reactants. When the fine C particles (e.g., C black) and coarse BN particles are used as the reactants, the reaction mechanism might be different from that described here, which needs a further study.

4. Conclusions

The TiC_xN_y and TiB_2 ceramics were synthesized by a combustion reaction using Ti, C and BN reactants and the following conclusions were drawn:

(1) The reaction mechanisms in the Ti–C–BN system during the SHS process are only moderately dependent on the C/(C + N) ratio. The primary reactions are the preferential formation of $TiN_{0.3}$ and TiN and then incorporation of the C atoms in TiN_x to form the titanium carbonitride solid solution. In the samples with the low C/(C + N) ratios, TiB forms prior to the TiC_xN_y phase while it turns over in the samples with high C/(C + N) ratio.
(2) The C/(C + N) ratio has a great influence on the reaction behaviors and the final compositions of the combustion products. With the increase in the C/(C + N) ratio in the reactants, the combustion temperature shows a zigzag tendency with the maximum value displaying at C/(C + N) = 0.5 and the minimum value at C/(C + N) = 0.7; the combustion wave velocity exhibits a similar variation tendency as did in the combustion temperature while the ignition delay time increases progressively.
(3) Both the TiC_xN_y and TiB_2 grains have small sizes of less than 1 μm in the products when the C/(C + N) ratio is lower than 0.5, while a sintered microstructure of the ceramic particles with a lager grain size is observed in the sample with C/(C + N) = 0.9.

Acknowledgments

This work is supported by The National Natural Science Foundation of China (No. 50531030) and The Ministry of Science and Technology of China (No. 2005CCA00300) as well as by The 985 Project-Automotive Engineering of Jilin University.

References

[1] H.A. Zhang, J.H. Yan, X. Zhang, S.W. Tang, Int. J. Refract. Met. Hard Mater. 24 (2006) 236–239.
[2] W. Lengauer, in: R. Riedel (Ed.), Handbook of Ceramic Hard Materials, vol. 1, Wiley–VCH, Weinheim, 2000, pp. 202–252.
[3] P. Ettmayer, H. Kolaska, W. Lengauer, K. Dreyert, Int. J. Refract. Met. Hard Mater. 13 (1995) 343–351.
[4] S. Zhang, Key Eng. Mater. 138–140 (1998) 521–543.
[5] S. Bolognini, G. Feusier, D. Mari, T. Viatte, W. Benoit, Int. J. Refract. Met. Hard Mater. 16 (1998) 257–268.
[6] S. Kang, Mater. Sci. Eng. A 209 (1996) 306–312.
[7] A. Bellosi, V. Medri, F. Monteverde, J. Am. Ceram. Soc. 84 (11) (2001) 2669–2676.
[8] F. Monteverde, V. Medri, A. Bellosi, J. Eur. Ceram. Soc. 22 (2002) 2587–2593.
[9] A. Jha, S.J. Yoon, J. Mater. Sci. 34 (2) (1999) 307–322.
[10] J. Xiang, Z. Xie, Y. Huang, H. Xiao, J. Eur. Ceram. Soc. 20 (2000) 933–938.
[11] A. Larsson, S. Ruppi, Thin Solid Films 402 (2002) 203–210.
[12] D. Carole, N. Fréty, S. Paris, D. Vrel, F. Bernard, R.-M. Marin-Ayral, Ceram. Int. 33 (2007) 1525–2534.
[13] C.L. Yeh, Y.D. Chen, Ceram. Int. 31 (2005) 719–729.
[14] R. Tomoshige, A. Murayama, T. Masushita, J. Am. Ceram. Soc. 80 (1997) 761–764.
[15] M. Eslamloo-Grami, Z.A. Munir, J. Mater. Res. 9 (2) (1994) 431–435.
[16] F. Olevsky, P. Mogilevsky, E.Y. Gutmanas, I. Gotman, Metall. Mater. Trans. A 27 (1996) 2071–2079.
[17] M. Shibuya, M. Ohyanagi, Z.A. Munir, J. Am. Ceram. Soc. 85 (12) (2002) 2965–2970.
[18] C.L. Yeh, G.S. Teng, J. Alloys Compd. 417 (2006) 109–115.
[19] X.H. Zhang, C. Yan, Z.Z. Yu, J. Mater. Sci. 39 (14) (2004) 4683–4685.
[20] Y.J. Liang, Y.C. Che, Notebook of Thermodynamic Data of Inorganic, East-North University Press, Sheng Yang, 1996.
[21] J.B. Holt, Z.A. Munir, J. Mater. Sci. 21 (1986) 251–259.
[22] Y.F. Yang, H.Y. Wang, J. Zhang, et al., J. Am. Ceram. Soc. 91 (2008) 2736–2739.
[23] Powder Diffraction File Card No. 32-1383 (CD ROM), International Center for Diffraction Data (ICDD), Newtown Square, PA.
[24] Powder Diffraction File Card No. 38-1420 (CD ROM), International Center for Diffraction Data (ICDD), Newtown Square, PA.
[25] L. Huang, H.Y. Wang, Q. Li, S.Q. Yin, Q.C. Jiang, J. Alloys Compd. 457 (1–2) (2008) 286–291.
[26] B.L. Zou, P. Shen, Q.C. Jiang, J. Mater. Sci. 42 (2007) 9927–9933.
[27] A.J. Horlock, D.G. Mccartney, P.H. Shipway, J.V. Wood, Mater. Sci. Eng. A 336 (2002) 88–98.
[28] X.L. Li, Fabrication of TiC Particulate Reinforced Magnesium Matrix Composites, Ph.D. Dissertation of the Jilin University, 2005.
[29] X.Y. Ma, C.R. Li, Z.M. Du, W.J. Zhang, J. Alloys Compd. 370 (2004) 149–158.